Molecular Therapy
Nucleic Acids
Original Article

Global characterization of RNA editing in genetic regulation of multiple ovarian cancer subtypes

Yulan Wang,[1,4] Jing Wu,[2,4] Jian Zhao,[1,4] Tianyi Xu,[3,4] Meng Zhang,[1] Jingjing Liu,[1] Yixuan Wang,[1] Quan Wang,[1] and Xiaofeng Song[1]

[1]Department of Biomedical Engineering, Nanjing University of Aeronautics and Astronautics, Nanjing 211106, China; [2]School of Biomedical Engineering and Informatics, Nanjing Medical University, Nanjing 211166, China; [3]National Genomics Data Center & CAS Key Laboratory of Genome Sciences and Information, Beijing Institute of Genomics, Chinese Academy of Sciences and China National Center for Bioinformation, Beijing 100101, China

RNA editing plays an extensive role in the initiation and progression of cancer. However, the overall profile and molecular functions of RNA editing in different ovarian cancer subtypes have not been fully characterized and elucidated. Here, we conducted a study on RNA editing in four cohorts of ovarian cancer subtypes through large-scale parallel reporting and bioinformatics analysis. Our findings revealed that RNA editing patterns exhibit subtype-specific characteristics within cancer subtypes. The expression pattern of ADAR and the number of differential editing sites varied under different conditions. CCOC and EOC exhibited significant editing deficiency, whereas HGSC and MOC displayed significant editing excess. The sites within the turquoise module of the coedited network also revealed their correlation with ovarian cancer. In addition, we identified an average of over 40,000 *cis*-edQTLs in the four subtypes. Finally, we explored the association between RNA editing and drug response, uncovering several potentially effective editing-drug pairs (EDP) and suggesting the conceivable utility of RNA editing sites as therapeutic targets for cancer treatment. Overall, our comprehensive study has identified and characterized RNA editing events in various subtypes of ovarian cancer, providing a new perspective for ovarian cancer research and facilitating the development of medical interventions and treatments.

INTRODUCTION

Ovarian cancer (OV) is a disease with clinical diversity and high histological and molecular heterogeneity,[1–3] and its histological phenotype is associated with distinct genetic patterns.[4] Each subtype has a different histopathology and a different response to treatment.[5,6] Based on histopathological examination, pathologists classify OV into high-grade serous OV (HGSC), low-grade serous OV (LGSC), clear cell OV (CCOC), endometrioid OV (EOC), and mucinous OV (MOC). While OV has traditionally been considered a singular disease, there is growing recognition that OV subtypes represent distinct diseases with diverse natural behaviors and prognoses.[7] These differences should be reflected in clinical study design and, ultimately, in the treatment of OV. However, the role of sequence variation caused by posttranscriptional events, such as RNA editing, in these diseases remains largely unexplored.

RNA editing is a widely recognized posttranscriptional modification mechanism that is catalyzed by adenosine deaminase acting on RNA (ADAR) enzymes.[8] This process involves altering the nucleotide sequence information of RNA molecules, typically through the insertion, deletion, or substitution of nucleotides. RNA editing can influence RNA splicing, protein recoding, microRNA binding, mRNA stability, and the biogenesis of circular RNAs,[9] thereby playing a crucial role in maintaining normal cellular functions, regulating gene expression in balance, and adapting to environmental changes. Studies have shown that RNA editing plays an important role in the pathogenesis of numerous diseases.[10] Researchers have extensively used quantitative trait locus (QTL) methods to discover genetic variations in molecular phenotypes, such as gene expression,[11,12] splicing,[13,14] and methylation.[15,16] RNA editing QTL (edQTL) analysis helps to elucidate disease-related genetic variants and their impact on editing levels, allowing for the prioritization of disease-causing editing sites. Recent investigations have focused on the relationship between RNA editing and genetic variation, particularly aberrant changes from adenosine to inosine (A-to-I). For example, RNA editing variability can affect the phenotype of complex traits and diseases by altering the stability and homeostatic levels of key RNA molecules.[17] Cuddleston et al. also investigated different brain regions linking spatiotemporal changes in cell type and editing levels to editing variation and genetic regulation.[18,19] Furthermore, RNA editing has been associated with drug resistance in tumors,[20] and ADAR1-mediated

Received 9 September 2023; accepted 18 January 2024;
https://doi.org/10.1016/j.omtn.2024.102127.

[4]These authors contributed equally

Correspondence: Quan Wang, Department of Biomedical Engineering, Nanjing University of Aeronautics and Astronautics, Nanjing 211106, China.
E-mail: wangquan@nuaa.edu.cn
Correspondence: Xiaofeng Song, Department of Biomedical Engineering, Nanjing University of Aeronautics and Astronautics, Nanjing 211106, China.
E-mail: xfsong@nuaa.edu.cn

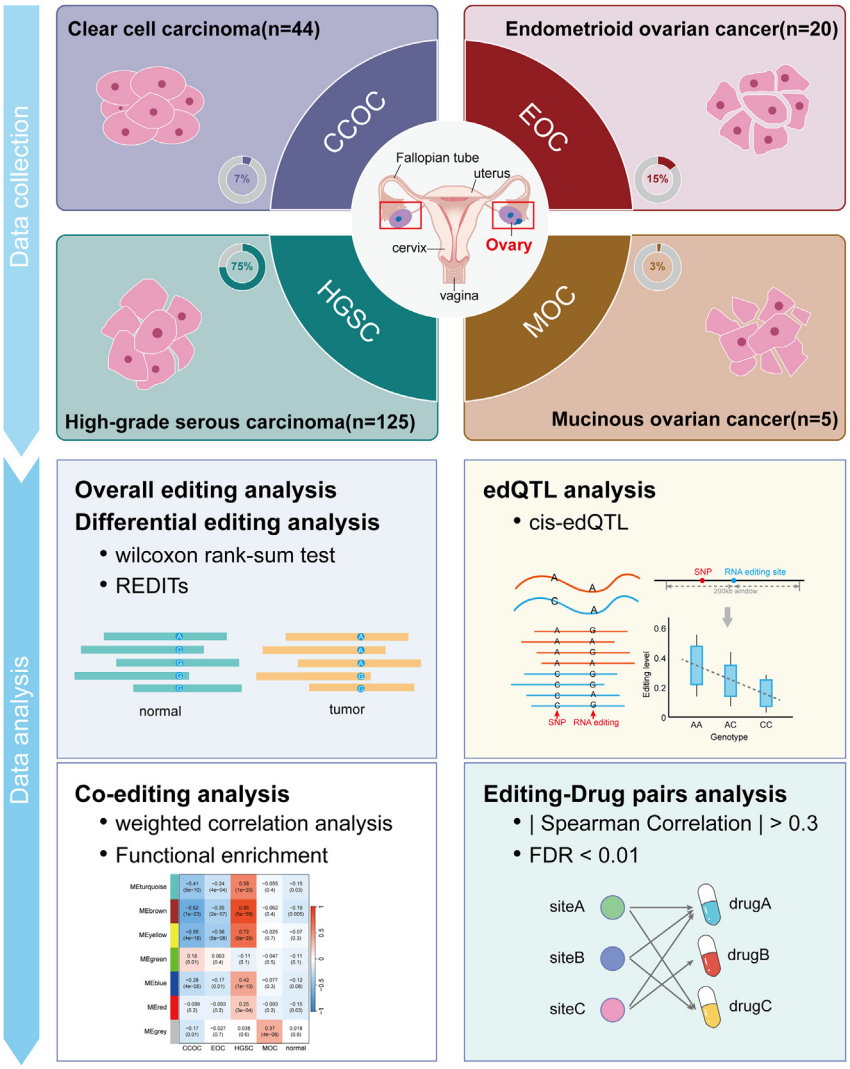

Figure 1. Schematic diagram of the analysis pipeline in this research

The donut chart and associated percentages represent the proportion of each OV subtype, and the colors represent different subtypes.

SCD1 RNA editing has been shown to drive drug resistance in gastric cancer.[21] Overall, the progression of OV is hindered by a combination of genetic and epigenetic changes, drug resistance, and increased genetic diversity in tumor cells. These factors present significant obstacles to achieving effective treatment. A-to-I RNA editing holds promise as a target for cancer immunotherapy.

In our previous study, we conducted an extensive exploration of RNA editing profiles in OV.[22] Given the heterogeneous nature of OV encompassing multiple subtypes, it is plausible that genetic variants may also govern A-to-I RNA editing. However, it is currently unclear whether differences or associations between RNA editing and the expression of different subtypes of OV can be attributed to specific biomarkers. Published studies have not thoroughly analyzed the mechanisms of RNA editing-mediated genetic regulation in OV. Therefore, a systematic analysis of A-to-I editing related to genetic variation and drug response is urgent and necessary.

We aimed to explore the possible links between altered RNA editing events and OV subtypes, providing a more comprehensive landscape of the genetic control of RNA editing in OV subtypes. To achieve this goal, here, we acquired 194 RNA sequencing (RNA-seq) datasets comprising four OV subtypes and 17 normal ovarian tissue samples. By integrating these datasets, we systematically elucidated the RNA editing events associated with OV subtypes. Our analysis encompassed not only the overall/differential editing (DE) but also the dissection of edQTL, co-edited networks, and RNA editing events associated with drug response (Figure 1). These results revealed an extensive repertoire of highly regulated RNA editing sites (RES) in different subtypes of OV and provided a resolved map linking OV subtypes with editing variation and genetic regulatory effects. In conclusion, our findings suggested that RNA editing plays a critical role in OV development and greatly deepen our understanding of RNA editing-mediated cancer development and therapy.

RESULTS

Subtype-specific characteristics of RNA editing patterns in OV

OV exhibits heterogeneity. However, the extent of RNA editing events among different subtypes remains largely unknown. In this study, we downloaded a total of 211 OV samples for analysis. A multistep approach was used to progressively identify RNA editing sites by integrating RNA-seq datasets and SNP information (Figure 2A; see Materials and methods). Stringent downstream filtering and quality control were applied to all of the sites. Overall, our analysis identified 216,669 (CCOC), 117,650 (EOC), 768,377 (HGSC), and 124,980 (MOC) editing sites within the four subtypes of OV samples, respectively, compared to 422,572 editing sites in normal samples (Figure 2B). Interestingly, a considerable proportion of these sites were located in repetitive sequences, with the majority (75%) attributed to Alu repeats. Furthermore, 73.87% of CCOC, 37.23% of EOC, 84.36% of HGSC, and 42.63% of MOC were classified as cancer subtype specific, indicating unique detection within a specific subtype (Figure 2B).

We thoroughly annotated all of the editing events and identified consistent features among them. Across the detected sites, we observed a total of 12 types of editing: GT, AC, CT, AG, GC, CA, AT, TG, GA, TA, TC, and CG, with the A-to-I being the most

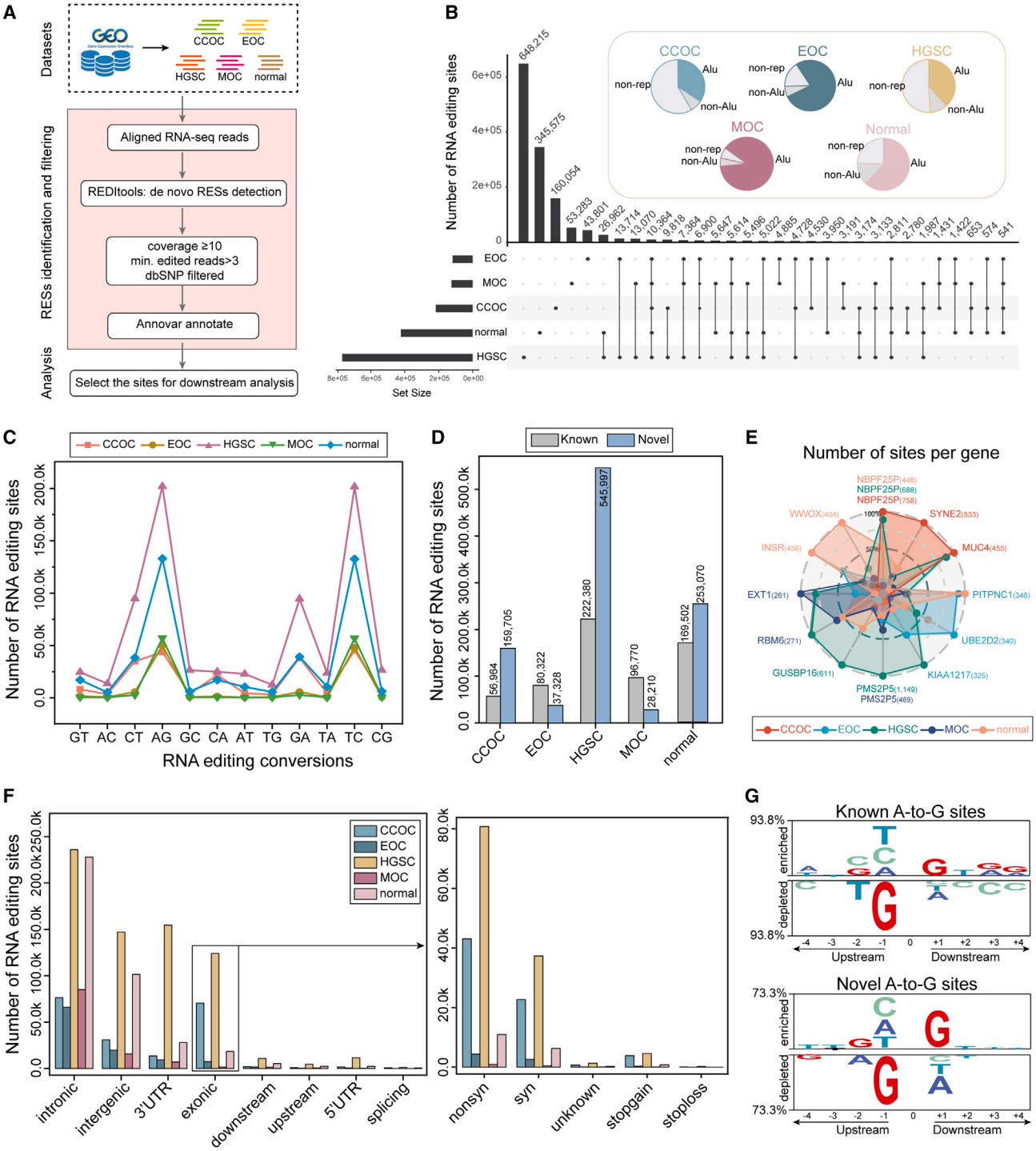

Figure 2. General characteristics of RNA editing events

(A) The workflow for detecting high-confidence OV subtype-associated editing sites, along with the *de novo* identification and filtering of RNA editing sites. (B) Upset plots displaying the counts and overlap of all subtype-enriched sites. The pie charts indicate the proportion of sites mapping to Alu elements compared to other elements. (C) Identification of different types of RNA editing. The x axis represents the editing type, and the y axis represents the total number of editing events. (D) The number of A-to-G editing sites (Y axis) categorized by annotations in the database (known or novel) and counted separately for each cancer subtype. (E) Spider plots showcasing the top 3 genes enriched with RNA editing sites for each cancer subtype. (F) Total number of RNA editing sites across genomic regions. (Right) Breakdown of coding regions. (G) Local sequence motif enrichment analysis of known and novel sites depicting the frequency of nucleotides in flanking sequences (upstream and downstream 4 bp) of G editing sites and randomly selected genomic "A" sites.

(legend continued on next page)

abundant in all 4 cancer subtypes (Figure 2C). In addition, we compared the RNA editing sites identified in this study with sites included in the REDIportal[23] database, which contains information on more than 4 million human A-to-I RNA editing sites. Our analysis revealed that 56,964 (26.29%, CCOC), 80,322 (68.27%, EOC), 222,380 (28.94%, HGSC), 96,770 (77.43%, MOC), and 169,502 (40.11%, control) A-to-I editing sites corresponded to known sites annotated in this database (Figure 2D). The sites identified in this study significantly expand the current knowledge of the editing landscape of OV subtypes. Most of the genes had multiple editing sites, with a notable correlation observed between the number of RNA editing sites per gene. Within CCOC, genes NBPF25P (n = 758 sites), SYNE2 (n = 533 sites), and MUC4 (n = 455 sites) were particularly enriched with editing sites. Studies have confirmed that MUC4 can be used as an independent marker for the early diagnosis of OV and can be used in combination with MUC16/CA125 to achieve higher sensitivity in the detection of advanced tumors.[24] In EOC, the genes PITPNC1 (n = 346 sites), UBE2D2 (n = 340 sites), and KIAA1217 (n = 325 sites) displayed enrichment of editing sites, whereas in HGSC, the genes PMS2P5 (n = 1,149 sites), NBPF25P (n = 688 sites), and GUSBP16 (n = 611 sites) exhibited enrichment. We found enrichment of editing sites in the genes PMS2P5 (n = 469 sites), RBM6 (n = 271 sites), and EXT1 (n = 261 sites) in MOC (Figure 2E). Conversely, the genes NBPF25P (n = 448 sites), INSR (n = 456 sites), and WWOX (n = 404 sites) were found in normal samples (Figure 2E). Notably, the PMS2P5 variant with the higher editing rate among the four subtypes was associated with OV. PMS2 variants have been associated with breast cancer and OV, with a frequency of up to 47.6%.[25] Approximately 80.99% of all of the editing events were found in introns, with only a small fraction (4.06%) affecting protein-coding regions (Figure 2F).

Although ADARs do not have strict sequence specificity, the enzyme does exhibit a preference for certain adjacent nucleotides in a position-dependent manner.[26] We used Two Sample Logos[27] to validate the presence of a common local sequence motif of 4 bp flanking all adenosine-to-guanine (A-to-G) editing events. Our analysis revealed a depletion of guanosine at −1 bp upstream of the target adenosine, whereas its enrichment was observed at +1 bp downstream (Figure 2G). Therefore, ADAR preference and selectivity are guided by the primary sequence and secondary structure (i.e., *cis*-acting regulatory elements) surrounding the editing site.

Differential expression patterns of ADAR in OV subtypes

A-to-I RNA editing is the most common editing event and is mediated by editing enzymes (ADAR1, ADAR2, ADAR3). Given that the majority of RNA editing occurs in Alu elements and that almost all adenosine in the Alu repeats are targets of ADAR, we investigated the expression levels of the three ADAR editing enzymes, along with the average expression levels in the three Alu families. Notably, all of the samples had been treated to eliminate batch effects (Figure S1). We observed that ADAR1 expression was significantly higher in HGSC compared to other cancer subtypes, with MOC displaying the lowest ADAR1 expression (Figure 3A). Overall, the expression of three editing enzymes in CCOC, EOC, and MOC was lower than that in normal samples, whereas HGSC had slightly higher expression levels compared to normal samples. Since ADAR1 mediates A-to-I RNA editing events, we further assessed the differences in RNA editing among OV subtypes by calculating the overall editing level (OEL) of each sample (Figures 3B and 3C). Interestingly, the global A-to-I editing level of each subtype was inconsistent with the expression pattern of ADAR1, with higher OELs in CCOC, HGSC, and MOC compared to normal samples, and the lowest editing rate in the EOC subtype. Furthermore, the expression of all three Alu families (AluJ, AluS, AluY) showed consistency (Figure 3D). Also, we calculated the recoding editing index (REI), which was calculated based on the weighted average of the editing levels of all of the known recoding sites in the REDIportal database. All OV subtypes exhibited a higher REI than normal samples (Figure 3E). Notably, changes in OEL were positively correlated with the expression of ADAR1 (R^2 = 0.01, p = 0.121), ADAR2 (R^2 = 0.01, p = 0.12), and ADAR3 (R^2 = 0.06, p = 0.00049) (Figure 3F).

Distinct patterns of differential editing in OV subtypes

Since RNA editing may be highly cancer subtype specific, we investigated whether the differential editing patterns in OV originate from specific cancer subtypes. To comprehensively detect differential editing sites (DESs) in each subtype, we used the REDIT and Wilcoxon rank-sum tests to calculate differential editing ($p < 0.05$ and mean editing level difference $|Diff| \geq 5\%$), subsequently intersecting the results. This analysis revealed 3,934 (CCOC), 835 (EOC), 2,477 (HGSC), and 5,994 (MOC) DESs between OV and control in each of the 4 OV cohorts. Overall, CCOC and EOC exhibited a tendency of underediting, whereas HGSC and MOC tended to overediting (Figures 4A–4D).

There was a minimal overlap between DESs in these subtypes (Figure 4E), indicating distinct editing patterns for each subtype. Most of the DESs were found in intronic regions, intergenic regions, and 3′ UTRs (Figure 4F). Only a limited number of DESs resulted in nonsynonymous amino acid changes, stop loss, or stop gain, which were classified as RNA recoding events. Specifically, we found 130 (54.39%, CCOC), 52 (57.78%, EOC), 50 (56.18%, HGSC), and 20 (52.63%, MOC) sites, respectively, which could lead to changes in the amino acid sequence (Figure 4G). Although editing events in coding regions are rare, these editing events may have important functions. Through a comprehensive evaluation of the impact of these nonsynonymous mutations using SIFT, PolyPhen-2, and PROVEAN in ANNOVAR,[28] we found that a total of 27 sites were classified as deleterious (Figure 4H). We demonstrated the amino acid substitutions caused by the synonymous DESs under each subtype condition in OV. In addition, the majority (85%) of these genes associated with OV were found among the 27 deleterious DESs (Figures 4I; Table S1). For example, the editing level of the NRP1 coding region was higher in EOC relative to normal samples. A previous study proposed that increased NRP1 expression may be associated with the development of EOC and that NRP1 could serve as a valuable

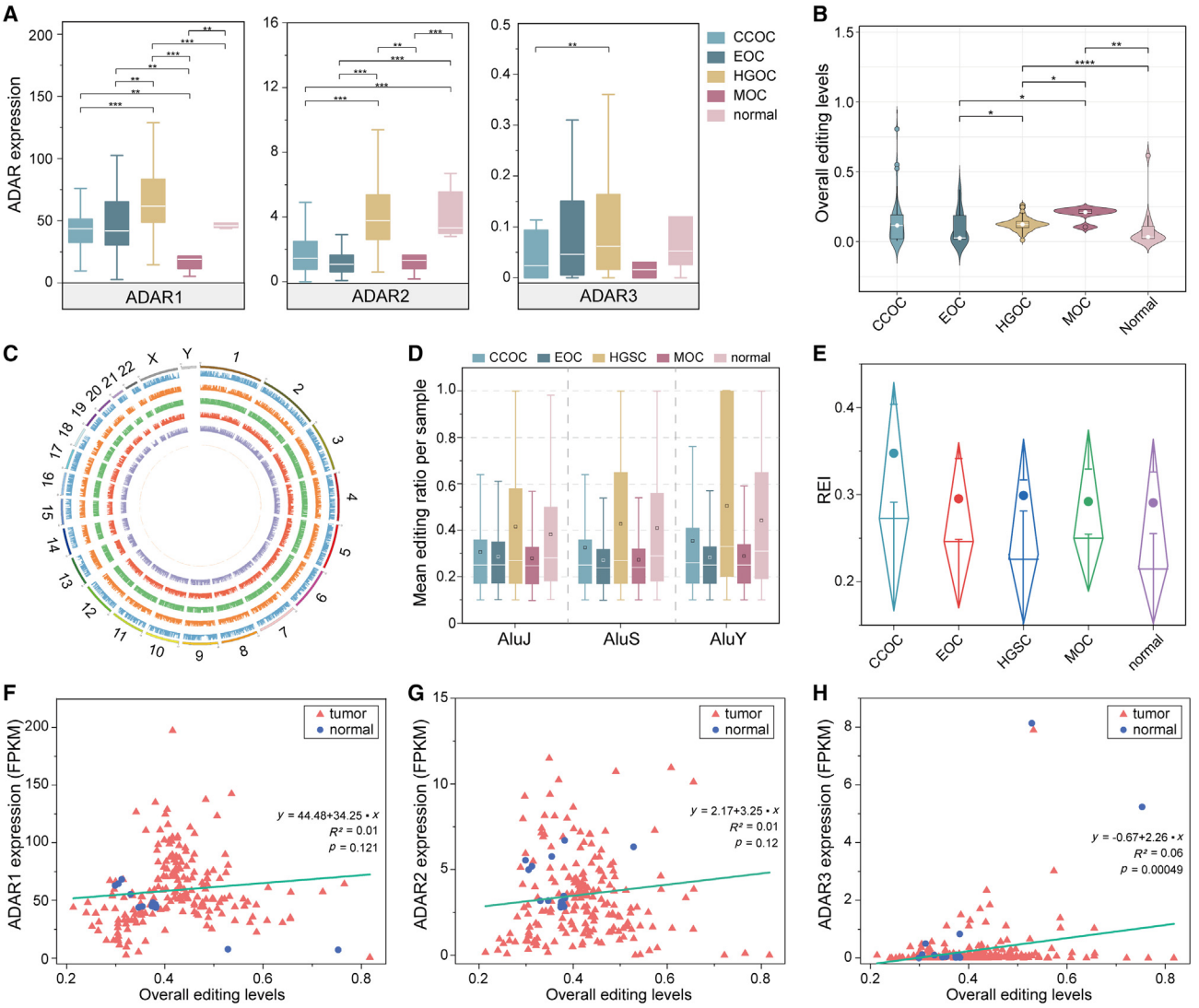

Figure 3. Transcriptome-wide overall RNA editing profiles across OV subtypes

(A) Estimation of mRNA expression levels of ADAR1, ADAR2, and ADAR3 in OV subtypes from RNA-seq data. The p value was measured by Wilcoxon rank-sum test. *p ≤ 0.05; **p ≤ 0.01; ***p ≤ 0.001. (B) Overall RNA editing levels for all cancer subtypes. Significance between groups was tested using the t test. Whisker box line plots display the median, lower quartile, and upper quartile, with whiskers representing the minimum and maximum values. (C) Circos plots of the genome-wide editing levels. (D) The boxplot of the mean editing ratios of the 3 major Alu subfamilies (S, Y, and J). (E) REI for all OV subtypes. (F–H) The correlation between (F) ADAR1 (R^2 = 0.01, p = 0.121), (G) ADAR2 (R^2 = 0.01, p = 0.12), and (H) ADAR3 (R^2 = 0.06, p = 0.00049) expression levels and OELs across all of the samples. FPKM, transcripts per kilobase per million mapped reads.

prognostic marker as well as a potential molecular therapeutic target for OV patients.[29]

Co-editing network modules and their correlation with OV

To further evaluate OV-related editing sites shared between OV subtype cohorts, we performed weighted gene coexpression network analysis (WGCNA)[30] on common RNA editing sites (see Materials and methods). The purpose of this analysis is to identify clusters of RNA editing sites (i.e., modules) that are associated with disease status. To ensure the stability and accuracy of the results, we must pay attention to the influence of outlier samples on the results (Figure S2). A soft threshold (β value) of 4 was determined for the coordinately edited (coedited) network (Figure S3) to ensure that the correlation matrix conformed to an approximate scale-free topology. For each cohort, WGCNA generated multiple modules (Figure 5A). Notably, we identified a module enriched in editing sites (labeled "turquoise" module), which was significantly associated with HGSC (Figure 5B). The editing sites in the turquoise modules in all of the cohorts have a high degree of overlap in the HGSC subtype (Figure 5C). These cohorts also shared a large number of genes containing editing sites

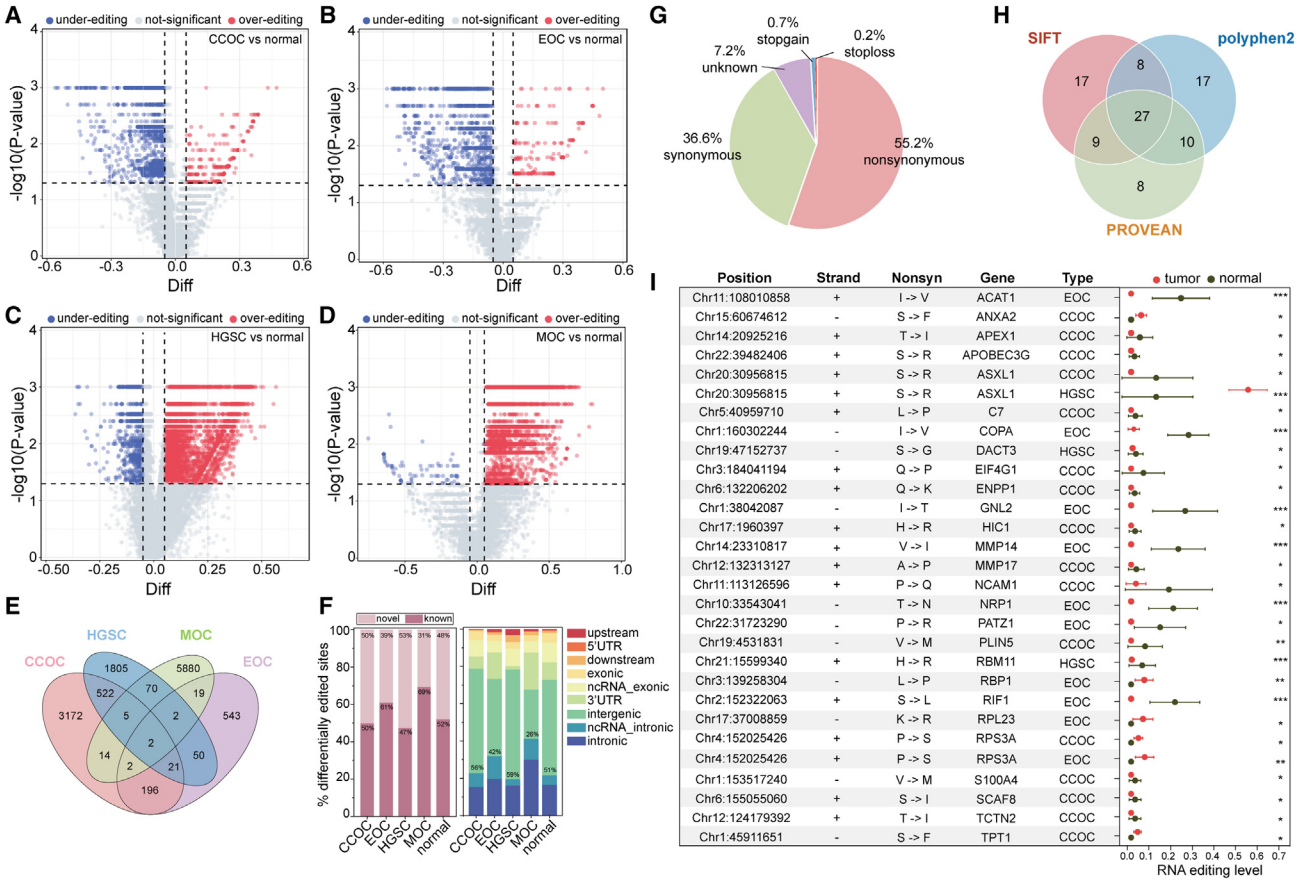

Figure 4. Identification and analysis of differential RNA editing in subtypes of OV

(A–D) Differential editing in (A) CCOC, (B) EOC, (C) HGSC, and (D) MOC. |Diff| represents the difference of the mean editing level between tumor and normal samples. (E) Venn diagram of DESs across all OV subtypes. (F) Annotation of all DESs. (G and H) Functional annotation of DESs. (I) Genes corresponding to differentially edited sites causing nonsynonymous mutations are associated with OV (*p ≤ 0.05; **p ≤ 0.01; ***p ≤ 0.001).

in the turquoise module. Gene Ontology (GO) analysis of the shared genes revealed a number of pathways associated with mitotic G2/M checkpoints, such as negative regulation of G2/M transition of the mitotic cell cycle, mitotic G2/M transition checkpoint, and mitotic G2 DNA damage checkpoint signaling (Figure 5D). OV is a multifactorial disease, and these malignancies are characterized by abnormal proliferation resulting from altered cell-cycle regulatory mechanisms.[31] Studies indicate that G2/M checkpoint inhibition and DNA damage often lead to mitotic catastrophe. Dysregulation of the cell-cycle regulation leads to increased cancer cell proliferation, and disruption of cell-cycle checkpoints, which is recognized as a hallmark of many cancers.[32,33] Therefore, aberrant regulation of these pathways may lead to cell-cycle disruption, accumulation of DNA damage, and inhibition of apoptosis, thereby promoting OV development and progression.

Association of RNA editing with genetic variants

To identify genetic variants that could explain selective RNA editing variability, we used estimated genotype data to test for common SNPs associated with RNA editing levels (edQTL, editing quantitative trait loci) (Figure 6A; see Materials and methods). We tested for association in each OV subtype and identified *cis*-edQTL at a genome-wide false discovery rate (FDR) <0.05 (i.e., restricting the analysis to SNPs within 200 kb upstream and downstream of the RES). A total of 21,869 (CCOC), 21,572 (EOC), 116,747 (HGSC), and 23,790 (MOC) *cis*-edQTL, respectively, were annotated. In addition, we compared the absolute effect sizes of all edQTLs and found that the HGSC subtype exhibited the lowest effect size, and MOC had the highest effect size (Figure 6F). We observed that variants within 1 megabase (MB) of the editing site were more likely to be significantly associated, and that each max-edQTL (defined as the most significant SNP-site pair per site, if any) that satisfied the genome-wide significance threshold was highly enriched within 200 kb of its associated editing site and acted in *cis* (Figure 6G). We examined the locations of edQTL editing sites (eSites) in genomic regions. The locations of these eSites were similar to common A-to-I editing sites, which were located mainly in introns (46%) as well as in the 3′ UTR (16%) (Figure 6H).

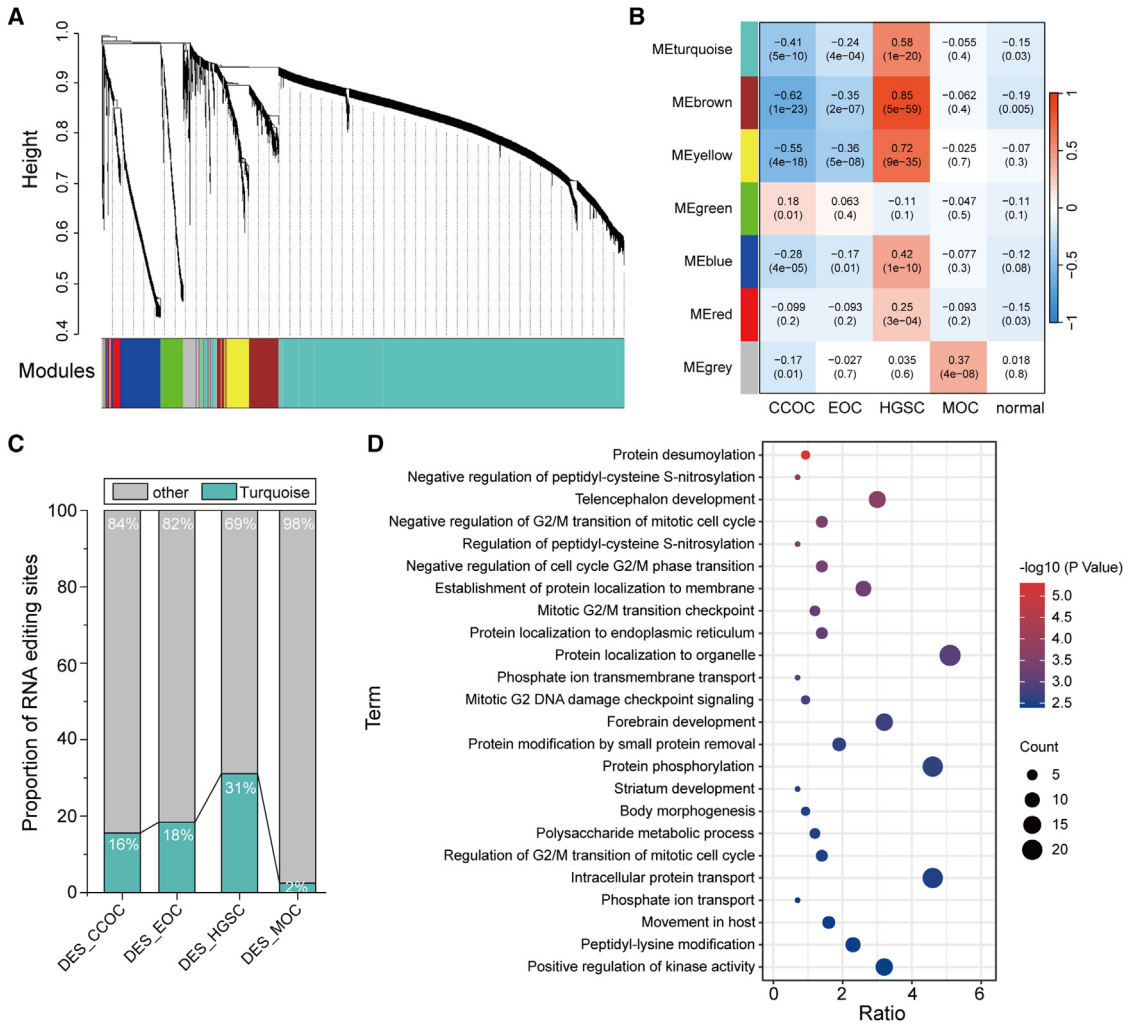

Figure 5. Unsupervised coedited network analysis of RNA editing in each subtype of OV

(A) Dendrogram of RNA editing sites. Each color represents different coedited modules, and turquoise modules are indicated by turquoise color. (B) Heatmap of the correlation of editing sites in different modules with different conditions (cancer or healthy tissue), and the numbers in the heatmap represent the coefficients and p values of the Pearson correlation. (C) Overlap between turquoise sites and differentially edited sites. (D) GO enrichment analysis of genes harboring turquoise sites (n = 473 genes).

To validate the edQTL, we compared the changes in the editing levels of eSites with the genotypes of the associated SNPs. We observed a significant correlation between the editing level of eSites and the genotypes of the associated SNPs. For example, for the chr7:63354367:AG edQTL in CCOC, the A allele at rs1408601915 was associated with high levels of RNA editing, whereas the G allele attenuated RNA editing (Figure 7B). The YWHAE (tyrosine 3-monooxygenase/tryptophan 5-monooxygenase activation protein epsilon) is a protein-coding gene. YWHAE can acts as an HE4-interacting protein that can influence the malignant behavior of OV by regulating the phosphatidylinositol 3-kinase (PI3K)/AKT and mitogen-activated protein kinase pathways.[34] YWHAE enhances invasion, migration, and proliferation, and inhibits apoptosis in OV cells.[34] Despite the correlation between YWHAE and YWHAEP1 genes, further studies are needed to elucidate their specific relationships and interactions.

Enrichment analysis of the genes corresponding to all edQTL-associated eSites resulted in significant enrichment into pathways associated with OV (Figure 7C). For example, the PI3K/AKT and AMPK signaling pathways play important roles in OV cell survival, metabolism, and proliferation. Adherens junctions and tight junctions, which are intercellular junctional structures, play important roles in cell-to-cell adhesion and the maintenance of cell polarity. Disturbed cytomembrane junctions may lead to decreased intercellular adhesion and loss of cell polarity, which are associated with OV development and metastasis.

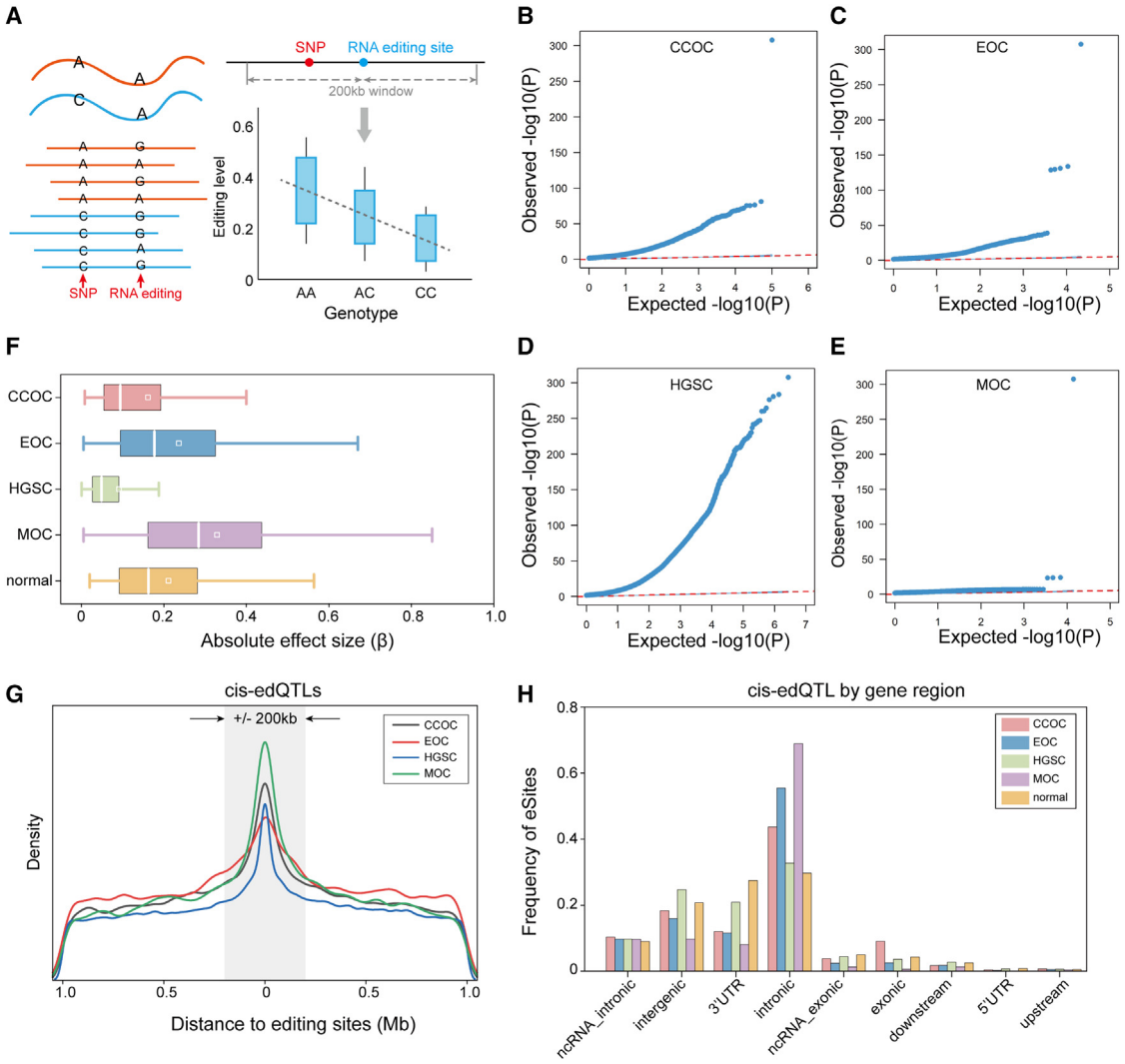

Figure 6. Characterization of RNA edQTL

(A) Schematic diagram of an edQTL. (B–E) Quantile-quantile plot for association tests between edQTL and RNA editing sites. (F) Comparison of the absolute effect sizes of edQTLs associated with cancer subtypes (β, x axis). (G) Distribution of the association tests in relation to the distance between the editing site and variant for *cis*-edQTLs. The gray box indicates ±200 kb relative to the editing site. (H) The total number of eSites (unique editing sites with associated edQTLs) categorized by gene region.

RNA editing as a potential therapeutic target for OV

We found editing-drug response associations in the data for all of the samples. Specifically, for each editing-drug pair (EDP), we measured rank associations using Spearman correlation and selected the EDP with the smallest associated p value (Figure 8A). In this study, we used IC_{50}, which is the concentration at which a substance inhibits certain biological programs to 50% inhibition. It can represent the degree of tolerance of a certain cell to a drug. The results yielded more than 10,000 EDPs, all of which were relatively significantly correlated (Figure 8B). Eventually, we screened the 10 most relevant EDPs and the corresponding drugs (Figures 8C; Table S2). It is worth noting that the NBPF gene plays an important role in OV. Itamochi et al. revealed that the most common mutations in 55 OV cases were NBPF20 (67%) and NBPF10 (60%), totaling 51 (93%) cases with mutations in NBPF20 and NBPF10, all of which were nonsynonymous mutations.[35] The host gene for the editing site (chr1:146034018) belongs to the NBPF family, and the nonsynonymous mutations generated by the editing may affect the occurrence and development of OV. The most relevant drug at this site is staurosporine. The experimental result of Alsamman et al. demonstrated that staurosporine treatment could lead to a significant reduction in p62 levels in OV and eliminate the cisplatin-induced upregulation of p62.[36] Staurosporine can sensitize OV cells to cisplatin through the mechanism of downregulation of p62.

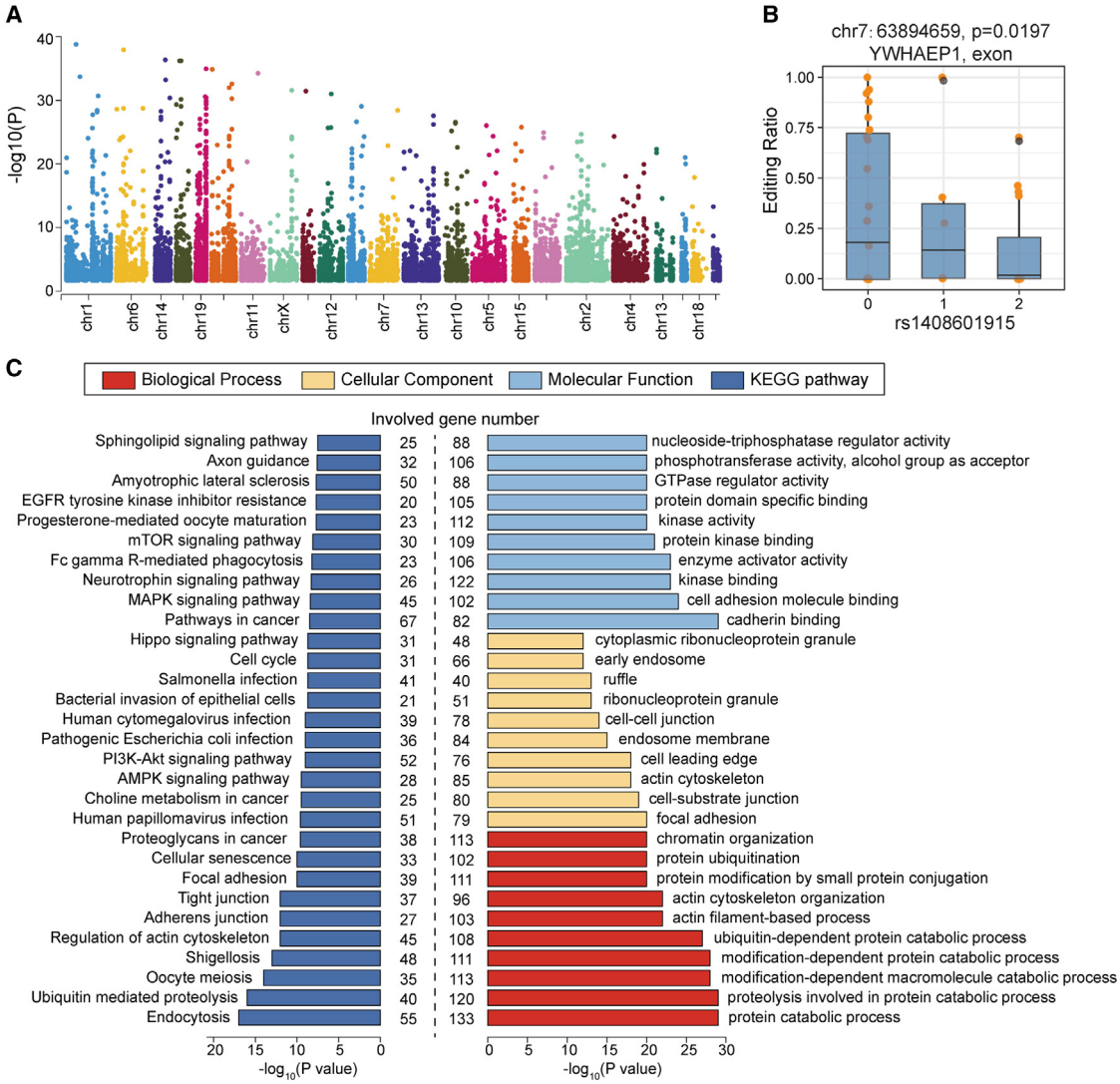

Figure 7. *cis*-edQTLs in OV subtypes

(A) Manhattan plot of the FDR for each A-to-I editing site in *cis*-edQTL mapping. (B) Examples of *cis*-eSites. Boxplots showing the association of editing levels with relevant SNP genotypes. (C) GO and Kyoto Encyclopedia of Genes and Genomes (KEGG) enrichment analysis of genes harboring the eSites (n = 1,823 genes). Red, biological process; yellow, cellular component; light blue, molecular function; dark blue, KEGG pathway. The numbers represent the number of genes involved in each item.

DISCUSSION

OV is the primary cause of gynecological cancer-related mortality and among the most prevalent fatal malignancies in women. Although 90% of tumors originate in the epithelium, OV exhibits considerable heterogeneity in clinical presentation and molecular biology.[37,38] RNA editing is one of the epigenetic mechanisms widely involved in the initiation and progression of various cancers. RNA editing holds promise as a diagnostic biomarker for associated diseases and is intricately linked to cancer prognosis. Recent recognition has highlighted common genetic variations as significant regulators of RNA editing levels.[18] Although numerous studies have explored RNA editing in cancer, the prevalence of RNA editing events across various subtypes of OV and the genetic determinants governing their regulation remain unclear. At present, limited studies have examined the correlation between this epigenetic modification, genetic regulation, and drug response. Given the scarcity of studies examining the comprehensive characteristics of RNA editing across various subtypes of OV, our primary aim was to assess the profile of RNA editing and its genetic regulation in four prominent OV subtypes.

In this study, we conducted the inaugural comprehensive analysis of RNA editing across subtypes of OV and identified distinct patterns in RNA editing among different subtypes. Within these subtypes, we identified genome-wide RNA editing sites and examined their genomic distribution. Consistent with previous studies, the majority of RNA editing sites were of the A-to-I type and primarily situated in noncoding

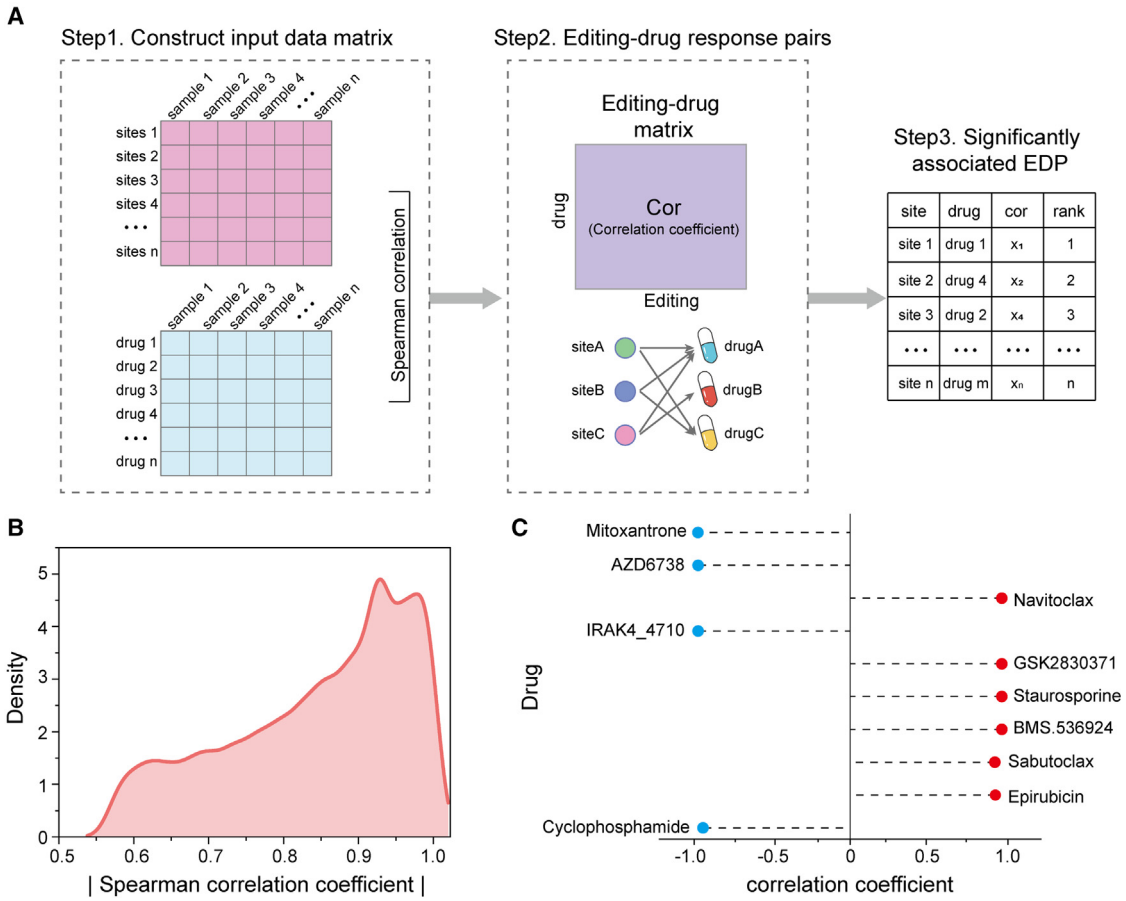

Figure 8. Identification of effective EDPs for OV treatment

(A) Simplified flowchart for identifying significantly correlated EDPs. (B) Distribution of Spearman correlation coefficients for significantly correlated EDPs. (C) The Spearman correlation coefficients of the drugs in the top 10 significantly correlated EDPs. Blue, significant negative correlation. Red, significant positive correlation.

regions, particularly in introns and 3′ UTRs. Interestingly, our findings revealed inconsistent expression patterns of ADARs across the four subtypes. Compared with normal samples, CCOC, HGSC, and MOC exhibited higher OEL, whereas the EOC subtype had the lowest editing rate. Among the recoding sites, all of the subtypes consistently exhibited higher REIs compared to controls. The differences in RNA editing levels among the different subtypes of OV may have an impact on subsequent gene expression and functional regulation. It may also lead to different pathological features and developmental patterns among OV subtypes, which is of significant importance for the diagnosis and treatment of the disease. There was a positive correlation observed within all of the cancer samples between the expression levels of ADAR and the overall A-to-I RNA editing levels.

Furthermore, we observed substantial diversity in the balance of overediting and underediting of DESs across various OV subtypes. CCOC and EOC demonstrated a propensity for underediting, whereas HGSC and MOC exhibited a proclivity for overediting. Studying the RNA editing patterns in different subtypes of OV contributes to a deeper understanding of the biological characteristics of tumors, their developmental patterns, and the development of personalized treatment plans. Specifically, we simultaneously observed 27 unique nonsynonymous DES variants across all four subtypes. A total of 85% of the genes harboring these variants were reported to be linked with the progression of OV. In addition, we conducted coedited network analysis in OV and identified coedited sites spanning across the subtypes. GO enrichment analysis of these sites revealed an association with the mitotic G2/M checkpoint as a top biological term. OV is a multifactorial disease, with numerous cell-cycle regulation irregularities playing a pivotal role in its occurrence and development. Also, we uncovered the prevalence of edQTLs in OV, with corresponding eSites primarily located in introns and 3′ UTR regions. The enrichment of these eSites also led to the enrichment of pathways significantly linked to OV. These findings expanded the landscape of RNA editing and its genetic regulation in OV. Finally, we also revealed the drug response mechanism mediated by RNA editing and screened potential drugs targeting RNA editing for the treatment of OV.

In conclusion, this study provides a comprehensive characterization of the RNA editing landscape in OV subtypes. These four subtypes

of OV exhibit distinct ADAR expression patterns and differential RNA editing (DRE) patterns (overediting and underediting). The edQTL analysis contributes to explaining the genetic variants linked to OV and their impact on editing levels. The identification of potentially effective editing-drug response pairs suggests that RNA editing sites could serve as promising therapeutic targets for cancer treatment.

Our study also had several limitations requiring further research. First, we did not consider LGSC among the multiple subtypes of OV that we studied. This absence could result in overlooking a distinct expression pattern in this subtype, potentially affecting the understanding of the developmental processes of OV. Second, our study lacked information on the colocalization of genome-wide association study loci and edQTL signatures in OV. This highlights the necessity for further exploration of edQTL signatures that colocalize with cancer loci in specific cancer types. Furthermore, although our study investigated the correlation between RNA editing and drug response, limited RNA editing and drug data confine our exploration to an initial stage. Therefore, future research holds promise for a more comprehensive understanding of the impact of RNA editing modifications on the mechanisms of resistance to anticancer therapies, potentially paving the way for personalized cancer therapy. In future research, the role of RNA editing at the single-cell level could be explored further. For example, using resources such as the single-cell transcription map available in the GEN[39] database could provide more in-depth insights into the distinct RNA editing attributes in OV.

MATERIALS AND METHODS

Data sources for OV subtypes

The RNA-seq datasets for each subtype of OV were obtained from the GEO (https://www.ncbi.nlm.nih.gov/geo/) database (Table S3). The cohort included a total of 194 OV samples, primarily comprising serous OV, CCOC, EOC, and MOC. However, HGSC predominated in the cohort, with LGSC samples being less common and excluded from the analysis. In addition, 17 normal ovarian tissue samples were collected for differential analysis. The utilization of multiple datasets may lead to technical variations, including RNA extraction, library preparation, and sequencing. These discrepancies could introduce variations in gene expression levels, potentially affecting the results of bioinformatics analysis. To address this issue, we used the combat-seq[40] method for RNA-seq data to remove batch effects.

RNA editing identification and annotation

The original FASTQ files were extracted from the sequence read archive by fasterq-dump (https://github.com/ncbi/sra-tools/wiki/HowTo:-fasterq-dump), a more efficient replacement for the old fastq-dump tool. Subsequently, the FASTQ datasets were aligned to the human reference genome (hg19) through hisat2[41] and samtools[42] with default parameters. Next, the REDITools[43] tool was used to identify RNA editing sites. To ensure the accuracy of the identified sites, several computational steps were performed: sites in the dbSNP were removed; sites required a minimum coverage of at least 10 reads and at least 3 edited reads. ANNOVAR[28] was used to annotate the functions and categories of the RNA editing sites. This tool provided annotations such as gene types of RNA editing sites and determined whether the editing sites would result in amino acid sequence changes.

Overall RNA editing

To determine the RNA editing status of each sample, we calculated the RNA editing level of each sample. The editing level was defined as the ratio of edited reads with G nucleotides at a given RNA editing site to the total reads at that site (i.e., total reads with A and G nucleotides). The derived metric is a continuous measure between 0 and 1, indicating a range from completely unedited (0) to completely edited (1).

DRE

DRE analysis was performed separately for each subtype cohort. To identify a set of high-quality and highly reliable DESs, we used two statistical methods in parallel and integrated their results to generate a comprehensive list of DESs. First, we used REDIT[44] software to identify RES with significantly DE levels between cancer and control. Second, we used the nonparametric Wilcoxon rank-sum test to detect RNA editing sites with divergent editing percentages between cases (OVs of each subtype) and controls (normal ovarian tissue). Finally, we combined the results of these two methods to identify the overlapping set of differential RNA editing sites.

WGCNA

To identify coedited sites in both OV and control samples, we applied an unsupervised WGCNA[30] method. WGCNA involved automated network construction and modular detection, facilitating the establishment of scale-free topology by setting corresponding soft-thresholds power. The sites that characterized each module were examined for correlation with the disease condition, aiming to identify the module exhibiting the highest correlation with the disease state. A linear regression model was used to evaluate this association.

edQTL analysis

To map genome-wide edQTLs, linear models were used to estimate genotype doses and levels of RNA editing using MatrixEQTL.[45] To emphasize the *cis*-regulatory role of the detected edQTLs, only SNPs within 200 kb of the edited site were included in the analysis. To control for multiple tests, the FDR was estimated for all *cis*-edQTLs (defined as the 200 kb between the SNP and the edited site). Significant *cis*-edQTLs were identified using a genome-wide significance threshold (FDR <0.05). For each editing site, the edQTL was defined as the closest SNP with the most significant MatrixEQTL p value.

RNA editing events related to drug response

Drug response data were obtained from the Genomics of Drug Sensitivity in Cancer,[46] which was developed by the Sanger Institute in the United Kingdom. We applied the method described by Ruan et al.,[47] performing a large-scale Spearman correlation test between RNA editing and drug response using the 'rcorr' function in the 'hmisc'

package. EDPs with an absolute Spearman correlation ≥ 0.3 and an FDR <0.01 were considered a significant association.

Function and pathway enrichment analysis

Functional annotation of genes with DESs was performed using Metascape[48] (http://metascape.org/) to conduct a comprehensive analysis of functional and pathway enrichment in the study. Metascape is a powerful online analysis website integrating gene annotation, functional enrichment analysis, and protein interaction analysis.

DATA AND CODE AVAILABILITY

All of the data that support the findings of this study are available from the corresponding authors upon reasonable request.

SUPPLEMENTAL INFORMATION

Supplemental information can be found online at https://doi.org/10.1016/j.omtn.2024.102127.

ACKNOWLEDGMENTS

This study was supported by grants from the National Natural Science Foundation of China (nos. 62273175 and 62003165), the Fundamental Research Funds for the Central Universities (no. NS2023017), and the Key R&D Projects of Jiangsu Province (no. BE2022843).

AUTHOR CONTRIBUTIONS

X.S. and Q.W. conceived the study and revised the manuscript. Y.W. implemented the study and drafted the manuscript. J.Z., J.W., and T.X. collected the public data, provided scientific advice, and contributed to the results interpretations. M.Z., J.L., and Y.W. provided technical support and performed the analysis. X.S., Q.W., and J.Z. assisted with manuscript review and revision. All of the authors read and approved the final manuscript.

DECLARATION OF INTERESTS

The authors declare no competing interests.

REFERENCES

1. Kopper, O., de Witte, C.J., Lõhmussaar, K., Valle-Inclan, J.E., Hami, N., Kester, L., Balgobind, A.V., Korving, J., Proost, N., Begthel, H., et al. (2019). An organoid platform for ovarian cancer captures intra- and interpatient heterogeneity. Nat. Med. *25*, 838–849. https://doi.org/10.1038/s41591-019-0422-6.

2. Piki, E., Dini, A., Raivola, J., Salokas, K., Zhang, K., Varjosalo, M., Pellinen, T., Välimäki, K., Veskimäe, K.T., Staff, S., et al. (2023). ROR1-STAT3 signaling contributes to ovarian cancer intra-tumor heterogeneity. Cell Death Dis. *9*, 222–310. https://doi.org/10.1038/s41420-023-01527-6.

3. Kossaï, M., Leary, A., Scoazec, J.-Y., and Genestie, C. (2018). Ovarian Cancer: A Heterogeneous Disease. Pathobiology *85*, 41–49. https://doi.org/10.1159/000479006.

4. O'Mahony, D.G., Ramus, S.J., Southey, M.C., Meagher, N.S., Hadjisavvas, A., John, E.M., Hamann, U., Imyanitov, E.N., Andrulis, I.L., Sharma, P., et al. (2023). Ovarian cancer pathology characteristics as predictors of variant pathogenicity in BRCA1 and BRCA2. Br. J. Cancer *128*, 2283–2294. https://doi.org/10.1038/s41416-023-02263-5.

5. Prat, J. (2012). Ovarian carcinomas: five distinct diseases with different origins, genetic alterations, and clinicopathological features. Virchows Arch. *460*, 237–249. https://doi.org/10.1007/s00428-012-1203-5.

6. Koshiyama, M., Matsumura, N., and Konishi, I. (2017). Subtypes of Ovarian Cancer and Ovarian Cancer Screening. Diagnostics *7*, 12. https://doi.org/10.3390/diagnostics7010012.

7. Köbel, M., Kalloger, S.E., Boyd, N., McKinney, S., Mehl, E., Palmer, C., Leung, S., Bowen, N.J., Ionescu, D.N., Rajput, A., et al. (2008). Ovarian Carcinoma Subtypes Are Different Diseases: Implications for Biomarker Studies. PLoS Med. *5*, e232. https://doi.org/10.1371/journal.pmed.0050232.

8. Nishikura, K. (2016). A-to-I editing of coding and non-coding RNAs by ADARs. Nat. Rev. Mol. Cell Biol. *17*, 83–96. https://doi.org/10.1038/nrm.2015.4.

9. Chalk, A.M., Taylor, S., Heraud-Farlow, J.E., and Walkley, C.R. (2019). The majority of A-to-I RNA editing is not required for mammalian homeostasis. Genome Biol. *20*, 268. https://doi.org/10.1186/s13059-019-1873-2.

10. Christofi, T., and Zaravinos, A. (2019). RNA editing in the forefront of epitranscriptomics and human health. J. Transl. Med. *17*, 319. https://doi.org/10.1186/s12967-019-2071-4.

11. Montgomery, S.B., Sammeth, M., Gutierrez-Arcelus, M., Lach, R.P., Ingle, C., Nisbett, J., Guigo, R., and Dermitzakis, E.T. (2010). Transcriptome genetics using second generation sequencing in a Caucasian population. Nature *464*, 773–777. https://doi.org/10.1038/nature08903.

12. Pickrell, J.K., Marioni, J.C., Pai, A.A., Degner, J.F., Engelhardt, B.E., Nkadori, E., Veyrieras, J.-B., Stephens, M., Gilad, Y., and Pritchard, J.K. (2010). Understanding mechanisms underlying human gene expression variation with RNA sequencing. Nature *464*, 768–772. https://doi.org/10.1038/nature08872.

13. Battle, A., Mostafavi, S., Zhu, X., Potash, J.B., Weissman, M.M., McCormick, C., Haudenschild, C.D., Beckman, K.B., Shi, J., Mei, R., et al. (2014). Characterizing the genetic basis of transcriptome diversity through RNA-sequencing of 922 individuals. Genome Res. *24*, 14–24. https://doi.org/10.1101/gr.155192.113.

14. Lappalainen, T., Sammeth, M., Friedländer, M.R., 't Hoen, P.A.C., Monlong, J., Rivas, M.A., Gonzàlez-Porta, M., Kurbatova, N., Griebel, T., Ferreira, P.G., et al. (2013). Transcriptome and genome sequencing uncovers functional variation in humans. Nature *501*, 506–511. https://doi.org/10.1038/nature12531.

15. Bell, J.T., Pai, A.A., Pickrell, J.K., Gaffney, D.J., Pique-Regi, R., Degner, J.F., Gilad, Y., and Pritchard, J.K. (2011). DNA methylation patterns associate with genetic and gene expression variation in HapMap cell lines. Genome Biol. *12*, R10. https://doi.org/10.1186/gb-2011-12-1-r10.

16. Gibbs, J.R., van der Brug, M.P., Hernandez, D.G., Traynor, B.J., Nalls, M.A., Lai, S.-L., Arepalli, S., Dillman, A., Rafferty, I.P., Troncoso, J., et al. (2010). Abundant quantitative trait loci exist for DNA methylation and gene expression in human brain. PLoS Genet. *6*, e1000952. https://doi.org/10.1371/journal.pgen.1000952.

17. Park, E., Jiang, Y., Hao, L., Hui, J., and Xing, Y. (2021). Genetic variation and microRNA targeting of A-to-I RNA editing fine tune human tissue transcriptomes. Genome Biol. *22*, 77. https://doi.org/10.1186/s13059-021-02287-1.

18. Cuddleston, W.H., Li, J., Fan, X., Kozenkov, A., Lalli, M., Khalique, S., Dracheva, S., Mukamel, E.A., and Breen, M.S. (2022). Cellular and genetic drivers of RNA editing variation in the human brain. Nat. Commun. *13*, 2997. https://doi.org/10.1038/s41467-022-30531-0.

19. Cuddleston, W.H., Fan, X., Sloofman, L., Liang, L., Mossotto, E., Moore, K., Zipkowitz, S., Wang, M., Zhang, B., Wang, J., et al. (2022). Spatiotemporal and genetic regulation of A-to-I editing throughout human brain development. Cell Rep. *41*, 111585. https://doi.org/10.1016/j.celrep.2022.111585.

20. Zhou, X., Mitra, R., Hou, F., Zhou, S., Wang, L., and Jiang, W. (2023). Genomic Landscape and Potential Regulation of RNA Editing in Drug Resistance. Adv. Sci. *10*, 2207357. https://doi.org/10.1002/advs.202207357.

21. Wong, T.-L., Loh, J.-J., Lu, S., Yan, H.H.N., Siu, H.C., Xi, R., Chan, D., Kam, M.J.F., Zhou, L., Tong, M., et al. (2023). ADAR1-mediated RNA editing of SCD1 drives drug resistance and self-renewal in gastric cancer. Nat. Commun. *14*, 2861. https://doi.org/10.1038/s41467-023-38581-8.

22. Wang, Y., Song, X., and Xu, T. (2021). Identification and Analysis of RNA Editing Events in Ovarian Serous Cystadenoma Using RNA-seq Data. Curr. Gene Ther. *21*, 258–269. https://doi.org/10.2174/1566523221666210211111324.

23. Mansi, L., Tangaro, M.A., Lo Giudice, C., Flati, T., Kopel, E., Schaffer, A.A., Castrignanò, T., Chillemi, G., Pesole, G., and Picardi, E. (2021). REDIportal: millions

of novel A-to-I RNA editing events from thousands of RNAseq experiments. Nucleic Acids Res. *49*, D1012–D1019. https://doi.org/10.1093/nar/gkaa916.

24. Chauhan, S.C., Singh, A.P., Ruiz, F., Johansson, S.L., Jain, M., Smith, L.M., Moniaux, N., and Batra, S.K. (2006). Aberrant expression of MUC4 in ovarian carcinoma: diagnostic significance alone and in combination with MUC1 and MUC16 (CA125). Mod. Pathol. *19*, 1386–1394. https://doi.org/10.1038/modpathol.3800646.

25. Espenschied, C.R., LaDuca, H., Li, S., McFarland, R., Gau, C.-L., and Hampel, H. (2017). Multigene Panel Testing Provides a New Perspective on Lynch Syndrome. J. Clin. Oncol. *35*, 2568–2575. https://doi.org/10.1200/JCO.2016.71.9260.

26. Eggington, J.M., Greene, T., and Bass, B.L. (2011). Predicting sites of ADAR editing in double-stranded RNA. Nat. Commun. *2*, 319. https://doi.org/10.1038/ncomms1324.

27. Vacic, V., Iakoucheva, L.M., and Radivojac, P. (2006). Two Sample Logo: a graphical representation of the differences between two sets of sequence alignments. Bioinformatics *22*, 1536–1537. https://doi.org/10.1093/bioinformatics/btl151.

28. Wang, K., Li, M., and Hakonarson, H. (2010). ANNOVAR: functional annotation of genetic variants from high-throughput sequencing data. Nucleic Acids Res. *38*, e164. https://doi.org/10.1093/nar/gkq603.

29. Jiang, H., Xi, Q., Wang, F., Sun, Z., Huang, Z., and Qi, L. (2015). Increased expression of neuropilin 1 is associated with epithelial ovarian carcinoma. Mol. Med. Rep. *12*, 2114–2120. https://doi.org/10.3892/mmr.2015.3580.

30. Langfelder, P., and Horvath, S. (2008). WGCNA: an R package for weighted correlation network analysis. BMC Bioinf. *9*, 559. https://doi.org/10.1186/1471-2105-9-559.

31. D'Andrilli, G., Kumar, C., Scambia, G., and Giordano, A. (2004). Cell Cycle Genes in Ovarian Cancer: Steps Toward Earlier Diagnosis and Novel Therapies. Clin. Cancer Res. *10*, 8132–8141. https://doi.org/10.1158/1078-0432.CCR-04-0886.

32. Barnaba, N., and LaRocque, J.R. (2021). Targeting cell cycle regulation via the G2-M checkpoint for synthetic lethality in melanoma. Cell Cycle *20*, 1041–1051. https://doi.org/10.1080/15384101.2021.1922806.

33. Cunningham, J.M., Vierkant, R.A., Sellers, T.A., Phelan, C., Rider, D.N., Liebow, M., Schildkraut, J., Berchuck, A., Couch, F.J., Wang, X., et al. (2009). Cell cycle genes and ovarian cancer susceptibility: a tagSNP analysis. Br. J. Cancer *101*, 1461–1468. https://doi.org/10.1038/sj.bjc.6605284.

34. Li, X., Wang, C., Wang, S., Hu, Y., Jin, S., Liu, O., Gou, R., Nie, X., Liu, J., and Lin, B. (2021). YWHAE as an HE4 interacting protein can influence the malignant behaviour of ovarian cancer by regulating the PI3K/AKT and MAPK pathways. Cancer Cell Int. *21*, 302. https://doi.org/10.1186/s12935-021-01989-7.

35. Itamochi, H., Oishi, T., Oumi, N., Takeuchi, S., Yoshihara, K., Mikami, M., Yaegashi, N., Terao, Y., Takehara, K., Ushijima, K., et al. (2017). Whole-genome sequencing revealed novel prognostic biomarkers and promising targets for therapy of ovarian clear cell carcinoma. Br. J. Cancer *117*, 717–724. https://doi.org/10.1038/bjc.2017.228.

36. Alsamman, K., and El-Masry, O.S. (2018). Staurosporine alleviates cisplatin chemoresistance in human cancer cell models by suppressing the induction of SQSTM1/p62. Oncol. Rep. *40*, 2157–2162. https://doi.org/10.3892/or.2018.6615.

37. Berek, J.S., and Bast, R.C. (2003). Epithelial Ovarian Cancer. In Holland-frei Cancer Medicine, 6th edition (BC Decker).

38. Prat, J. (2012). New insights into ovarian cancer pathology. Ann. Oncol. *23*, x111–x117. https://doi.org/10.1093/annonc/mds300.

39. Zhang, Y., Zou, D., Zhu, T., Xu, T., Chen, M., Niu, G., Zong, W., Pan, R., Jing, W., Sang, J., et al. (2022). Gene Expression Nebulas (GEN): a comprehensive data portal integrating transcriptomic profiles across multiple species at both bulk and single-cell levels. Nucleic Acids Res. *50*, D1016–D1024. https://doi.org/10.1093/nar/gkab878.

40. Zhang, Y., Parmigiani, G., and Johnson, W.E. (2020). ComBat-seq: batch effect adjustment for RNA-seq count data. NAR Genom. Bioinform. *2*, lqaa078. https://doi.org/10.1093/nargab/lqaa078.

41. Kim, D., Paggi, J.M., Park, C., Bennett, C., and Salzberg, S.L. (2019). Graph-based genome alignment and genotyping with HISAT2 and HISAT-genotype. Nat. Biotechnol. *37*, 907–915. https://doi.org/10.1038/s41587-019-0201-4.

42. Li, H., Handsaker, B., Wysoker, A., Fennell, T., Ruan, J., Homer, N., Marth, G., Abecasis, G., and Durbin, R.; 1000 Genome Project Data Processing Subgroup (2009). Genome Project Data Processing Subgroup (2009). The Sequence Alignment/Map format and SAMtools. Bioinformatics *25*, 2078–2079. https://doi.org/10.1093/bioinformatics/btp352.

43. Picardi, E., and Pesole, G. (2013). REDItools: high-throughput RNA editing detection made easy. Bioinformatics *29*, 1813–1814. https://doi.org/10.1093/bioinformatics/btt287.

44. Tran, S.S., Zhou, Q., and Xiao, X. (2020). Statistical inference of differential RNA-editing sites from RNA-sequencing data by hierarchical modeling. Bioinformatics *36*, 2796–2804. https://doi.org/10.1093/bioinformatics/btaa066.

45. Shabalin, A.A. (2012). Matrix eQTL: ultra fast eQTL analysis via large matrix operations. Bioinformatics *28*, 1353–1358. https://doi.org/10.1093/bioinformatics/bts163.

46. Yang, W., Soares, J., Greninger, P., Edelman, E.J., Lightfoot, H., Forbes, S., Bindal, N., Beare, D., Smith, J.A., Thompson, I.R., et al. (2013). Genomics of Drug Sensitivity in Cancer (GDSC): a resource for therapeutic biomarker discovery in cancer cells. Nucleic Acids Res. *41*, D955–D961. https://doi.org/10.1093/nar/gks1111.

47. Ruan, H., Li, Q., Liu, Y., Liu, Y., Lussier, C., Diao, L., and Han, L. (2022). GPEdit: the genetic and pharmacogenomic landscape of A-to-I RNA editing in cancers. Nucleic Acids Res. *50*, D1231–D1237. https://doi.org/10.1093/nar/gkab810.

48. Zhou, Y., Zhou, B., Pache, L., Chang, M., Khodabakhshi, A.H., Tanaseichuk, O., Benner, C., and Chanda, S.K. (2019). Metascape provides a biologist-oriented resource for the analysis of systems-level datasets. Nat. Commun. *10*, 1523. https://doi.org/10.1038/s41467-019-09234-6.